

Article

Smoky Wood-Fired Ancient Glass Furnaces: Carbon Analysis of Roman Glass by 2.0 MeV Deuteron Activation Technique

Chaturvedula S. Sastri ^{1,*}, Thierry Sauvage ², Olivier Wendling ², Aurélien Bellamy ² and Christian Humburg ³¹ Independent Researcher, Michael-Müller Ring 29, 55128 Mainz, Germany² CNRS-CEMHTI, Orléans University, 3A, Rue de la Ferrollerie, 45071 Orleans, Cedex 2, France³ Independent Researcher, Zeppelinstr. 25, 55131 Mainz, Germany

* Correspondence: c.sastri@t-online.de

Abstract: To understand the wood-fuel contamination problems faced by the ancient glass industry, some Roman glass fragments and beads were analysed for carbon by the elegant, non-destructive deuteron activation technique based on C-12(d,n)N-13 nuclear reaction. Carbon was found in all analysed glasses, covering a mass concentration range from 160 ppm to 2.2%, indicating that some fuel contamination was present in all samples. The higher concentration of 0.94 to 2.2% observed in some beads indicates that carbon was added intentionally as a “component” to the glass melt to obtain an amber colour.

Keywords: wood-fuel contamination; ancient glass furnaces; deuteron activation analysis; carbon determination in glass; positron emission; gamma-ray spectroscopy; decay curve analysis

1. Introduction

Romans were highly skilled in making glass, and their products were sold all over the ancient world. Their glass objects were functional, and, with their complex designs and patterns, were pieces of extreme beauty. Modern glass owes a lot to the technology developed by Romans. Due to the great impact of Roman glass on our modern society, it would be interesting to know what types of technical and maintenance problems the great masters had to deal with in making those wonderful works of art.

Some laboratories across Europe make Roman glass using the old recipes on special occasions. The glass makers Taylor and Hill, who have built several Roman-style furnaces, have provided full details of furnace construction and operation [1,2]. For construction, the interior design of the furnace with proper exit points for waste gases is very important. They observed that fuel gases became partly absorbed in the glass melt during operation. Also, if the molten glass is retained for a longer time in the furnace, the powdery residues from the furnace walls become absorbed in the melt. The fuel consumption rate (wood in kg/hour) of the furnace depends on the type of wood, like ash, beech, or green wood, used. It was found from a study of wood types indigenous to central Europe that the fuel gas emissions, like fine particles (PM), carbon dioxide (CO₂), carbon monoxide (CO), volatile organic compounds (VOC), and total hydrocarbons (THC), depend crucially on fuel type, combustion technology, combustion type, etc. [3,4]. This means that, as the ancient glass workshops depended very much on the locally available wood, the magnitude of fuel contamination could have been different from place to place depending on the type of wood used.

Lauemann et al. [5] have found from their studies on Roman-style furnaces that beech wood produced more ash than spruce and pine. They also noticed small mishaps taking place sometimes, like cracking of crucibles, leakage of molten glass through the cracks, and its mixing with ash at the furnace bottom. Glass makers at Villa Borg, Saarland, Germany have discussed the technical problems faced in the production of Roman mosaic glass, window glass, and glass beads [6].



Citation: Sastri, C.S.; Sauvage, T.; Wendling, O.; Bellamy, A.; Humburg, C. Smoky Wood-Fired Ancient Glass Furnaces: Carbon Analysis of Roman Glass by 2.0 MeV Deuteron Activation Technique. *Minerals* **2023**, *13*, 1001. <https://doi.org/10.3390/min13081001>

Academic Editors: Donatella Barca and Natalia Rovella

Received: 20 June 2023

Revised: 13 July 2023

Accepted: 26 July 2023

Published: 28 July 2023



Copyright: © 2023 by the authors. Licensee MDPI, Basel, Switzerland. This article is an open access article distributed under the terms and conditions of the Creative Commons Attribution (CC BY) license (<https://creativecommons.org/licenses/by/4.0/>).

According to Taylor and Hill [1], it is necessary to undertake daily maintenance, like removal of ash and charcoal from the fire-chamber, every morning before starting glass production. It was very unlikely that the ancient skilled masters followed uniform maintenance procedures at all their production units, and some might have given priority to other issues facing their centres, which would again mean the possibility of another source of serious carbon contamination at some centres.

There are some additional factors that can lead to carbon contamination. To reduce the melting temperature of sand, natron and plant ash (e.g., *Salsola*, *Salicornia*) fluxes were used in the ancient times [7,8]. The plant ash may contain small amounts of charcoal in the ash. Further, to produce a specific colour like amber, carbon was intentionally added to glass melt to provide reducing conditions throughout production time [9–11].

So, although glass is essentially a mixture of oxides like SiO_2 , Na_2O , MgO , Al_2O_3 , and CaO , there are many ways that carbon can enter molten glass, and, if we have a method to determine this carbon, we can obtain new information hitherto unknown about Roman furnaces. The carbon presence could be for reasons like faulty design of a furnace, preventing proper escape of waste gases, absence of proper maintenance of the furnace and its working place, utilising locally available “smoky” wood with higher gas emissions, etc. It was known that glass industries were “fuel hungry” and there were problems with fuel supplies to make quality glass in the later Roman period [12]. All these factors can contribute varying amounts of carbon. One of these or a combination of many factors could be the reason for any carbon observed in archaeological glass.

Further, if we detect excess carbon in amber and related coloured glasses, it would confirm the assumption that the ancient experts had used “organic materials or smoke from combustion” to create a reducing atmosphere and obtain the desired colours [11].

Carbon analysis in glass is a very difficult task, and standard techniques like Induction Coupled Plasma-Optical Emission Spectroscopy (ICP-OES), Induction Coupled Plasma-Mass Spectrometry (ICP-MS), X-ray Fluorescence (XRF), Electron Probe Micro Analysis (EPMA), Particle-Induced X-ray Emission (PIXE), Particle-Induced Gamma-ray Emission (PIGE), and Neutron Activation Analysis (NAA), are not suitable. Photon activation [13] is one possibility, but, glass being a complex material of several oxides, it may require chemical separation of the product radionuclide after irradiation. Deuteron-induced PIGE studies of carbon in steel samples are known [14], but, because of very low detection efficiency of high-energy gamma rays (3.1 MeV) and very high gamma-ray background in the experimental area, trace analysis of carbon in a complex material like glass may not be possible.

Charged Particle Activation Analysis (CPAA) is a well-known technique for the analysis of light elements like Li, B, C, N, and O [15–19] in high-tech materials. Our laboratory in Orleans has specialized in this area since the 1970s using various techniques, like PIXE, PIGE, RBS (Rutherford Backscattering), NRA (Nuclear Reaction Analysis), NAA, and CPAA. Recently, we have extended CPAA to archaeological samples and demonstrated the usefulness of 12 MeV proton activation for the analysis of 14 elements in archaeological glasses and pottery [20].

The most widely used application of charged particle activation, especially with protons and deuterons, today is in the production of radioisotopes required in nuclear medicine (example: PET imaging nuclides C-11, N-13, O-15, F-18, etc.) for diagnosis and therapy [21,22].

Among the various charged particles, Deuteron Activation Analysis (DAA), a branch of CPAA, known for over 70 years, is unique for carbon, permitting analysis at the parts-per-billion (ppb) level, mostly by pure non-destructive techniques in semiconductor materials, pure metals, etc. [16,23–27]. The reason for this high sensitivity is the reaction C-12(d,n)N-13 has at a high activation cross-section of nearly 170 mbarns already at 2.0 MeV [28].

In our recent publications, we demonstrated the usefulness of DAA for the analysis of carbon, sodium, magnesium, and aluminium in archaeological glasses and pottery [29–31]. DAA is a very sensitive and non-destructive technique, and all four of these elements can

be determined simultaneously in one analysis. A major advantage of DAA is that, although it is a nuclear technique, because of low energy and currents used for analysis, there will be no radiation damage to the samples, and they are safe for returning to the owner.

The aim of the current investigation is twofold. First, although Romans were skilled experts in making glass, their workplaces could not have been very “tidy and clean” as judged by modern standards. With wood as fuel, various problems might have occurred. As described above, the quality of glass production will be reflected from the carbon levels found in the products. By analysing different Roman glasses applying deuteron activation, which is an excellent analytical technique for carbon, one can obtain new insights into this problem and also its magnitude, which could again be different from region to region. Secondly, the glass beads in this study have been carefully selected to represent amber and related colours to verify, as suggested by some specialists, if carbon was added by the ancient experts as a component in higher amounts to the glass melt to maintain a reducing atmosphere and obtain the desired colours.

2. Experimental

2.1. Sample Collection and Preparation

The samples analysed are shown in Figure 1a,b. G1 and G2 are Roman glasses from Moguntiacum (Mainz), which was a military base under Roman rule. Small pieces were cut from the glasses for analysis.

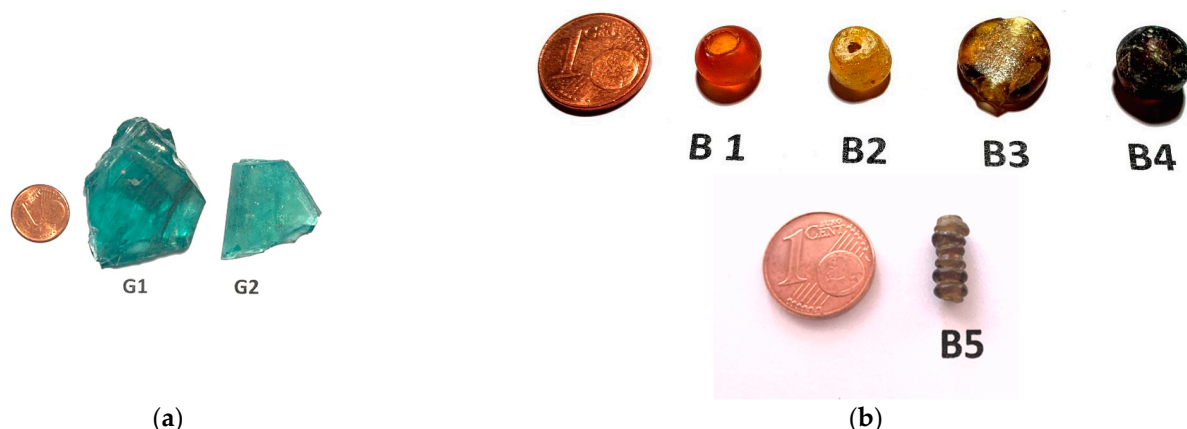


Figure 1. (a) Images of glass fragments G-1 and G-2 (small pieces were cut for analysis). (b) Images of glass beads—B1, B2, B3, B4, and B5.

B1 to B5 (Figure 1b) are Roman glass beads of different sizes (9 to 12 mm), and, with the exception of B4, which came from Mediterranean, others were collected from central and southern Europe, but their exact locations are not known.

All glasses were cleaned in distilled water and air-dried.

2.2. Standards

Thin metal foils of high purity were used as standards for Al (>99.9%) and Mg (>99.5%). Na was irradiated as a pellet of NaCl (analytical grade). High-purity carbon was irradiated as a piece of glassy carbon.

2.3. Method

With low-energy deuteron activation, the nuclear reaction useful for carbon analysis is shown in Table 1. The quoted half-lives are taken from Chu et al. [32]. As N-13 is a positron emitter (511 keV), its measurement can be interfered by other positron emitters generated by silicon and oxygen, which are actually main components of glass. So, the nuclear reactions induced on Si and O are also included in Table 1.

Table 1. Nuclear reactions with deuterons on carbon, sodium, magnesium, aluminium, oxygen, and silicon.

Element	Isotope	Abundance (%)	Nuclear Reaction	Product Nuclide Half-Life	Major γ -Rays (keV)
C	C-12	98.90	C-12(d,n)N-13	9.965 min	511
Na	Na-23	100	Na-23(d,p)Na-24	14.959 h	1368
Mg	Mg-26	11.01	Mg-26(d,p)Mg-27	9.458 min	844
Al	Al-27	100	Al-27(d,p)Al-28	2.2414 min	1779
O	O-16	99.76	O-16(d,n)F-17	64.49 s	511
	O-17	0.038	O-17(d,n)F-18	109.77 min	511
Si	Si-28	92.23	Si-28(d,n)P-29	4.14 s	511
	Si-29	4.67	Si-29(d,n)P-30	2.498 min	511

2.4. Analysis of Na, Mg, and Al

As mentioned in the introduction, DAA is sensitive also for Na, Mg, and Al, and any irradiation completed for carbon analysis also provides the results for these elements simultaneously. Hence, the nuclear reactions on these elements are also included in Table 1.

2.5. Comparison of DAA and PIGE

As many archaeologists are familiar with PIGE technique, we would like to briefly compare both the techniques here. DAA can be implemented in any laboratory with PIXE/PIGE facilities. DAA is as simple as PIGE, and, in Orleans, we use a PIGE setup to complete DAA (Figure 2a). However, there are some important differences: (1) nuclear reactions used for both techniques are very different. (2) PIGE involves measurement of “prompt” radiation at the irradiation site itself where the gamma-ray background will be high due to beam interaction with metallic (mostly tantalum) slits in front of the target used to adjust the beam size, interaction of scattered beam with the beam line, interaction of secondary neutrons with surrounding wall material of accelerator room, etc.

DAA involves “delayed” measurements where the counting of induced radioactivity is completed in a separate room. In Orleans, the counting is completed in a low-background room, with a Pb-shielded High Purity Germanium (HPGe) detector (Figure 2b), resulting in much lower background and improved signal to background ratios for the measured gamma rays. Because of this efficient shielding, the high-gamma-ray background observed in PIGE experiments is not present in DAA. Also, the contribution to 511 keV peak from positron emitters from natural background of U and Th series present in the construction materials of the walls of the counting room is found to be negligible. Further, the sample is placed directly on top of the HPGe detector in contact with detector-head, leading to higher efficiency in detection.

In DAA, similar to PIXE and PIGE, only a thin layer on the glass surface (ca. 20 microns thickness) becomes irradiated with 2.0 MeV deuterons. As the irradiated glass specimen can be several millimetres thick, it is important to see that this irradiated surface directly faces the detector while counting to prevent self-absorption of gamma rays within the sample thickness. Further, as the counting in DAA includes short-lived nuclides like Al-28, it is necessary to start the counting as soon as possible, with minimum delay after completing an irradiation.

2.6. Irradiations and Counting

The irradiations were performed with 2.0 MeV deuterons at the pelletron accelerator of CNRS-CEMHTI, Orleans. The glass samples were irradiated for 10 min at a current of 20 to 30 nA. Na, Mg, and Al standards were irradiated for 10 min at 10 to 20 nA. Carbon standard was irradiated at 5 nA for 5 min. The beam size for irradiations was 2.0×2.0 (mm \times mm).

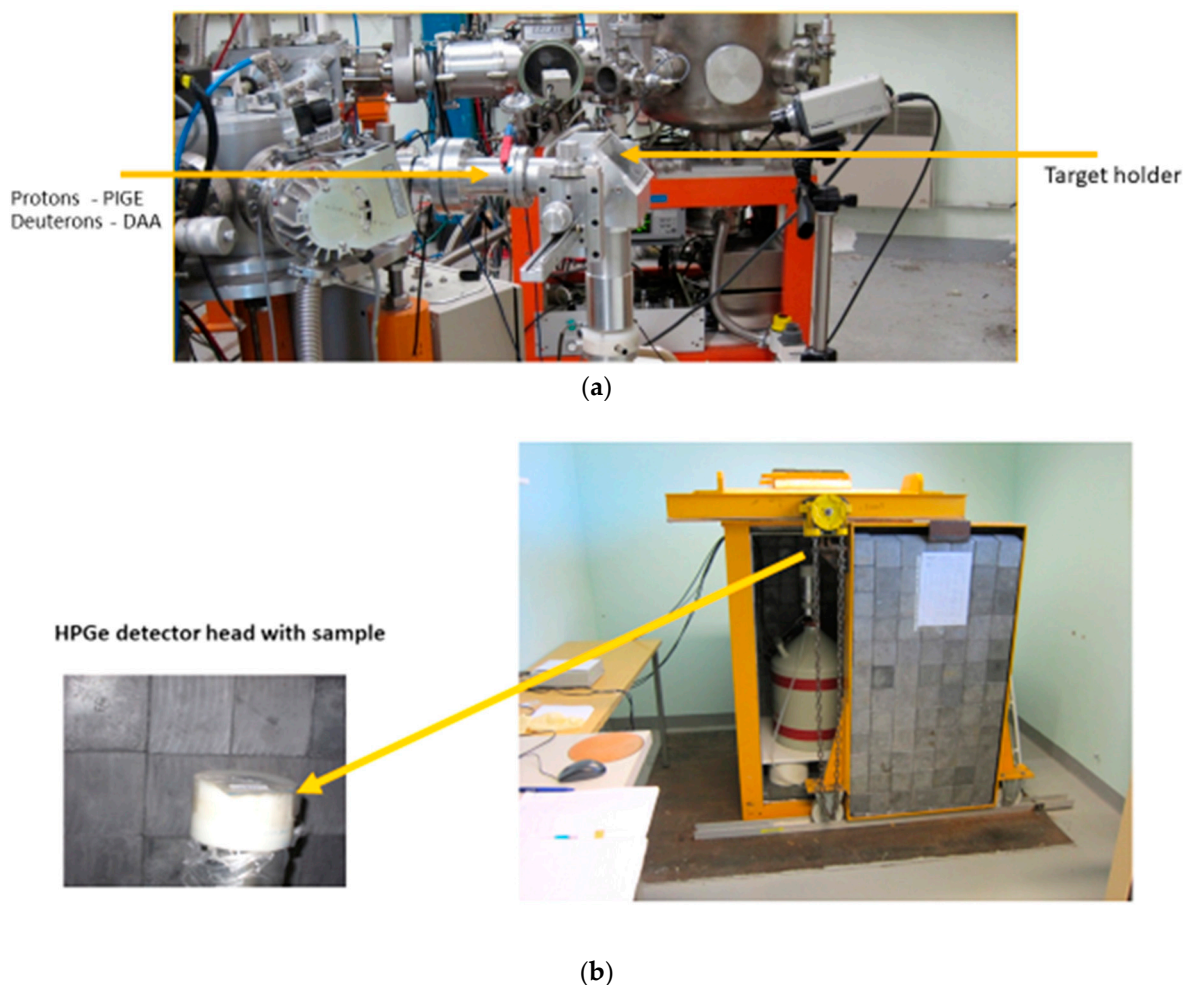


Figure 2. (a) PIGE/DAA setup at CNRS-CEMHTI. (b) Counting of DAA samples at CNRS-CEMHTI with HPGe detector, placed inside a low-background Pb-chamber, with a sliding door (sample is packed in a small plastic bag and placed at the centre on detector head. Sample transfer time from pelletron to counting room: 6 to 8 min).

After irradiation, the samples/standards were packed in small plastic bags and counted with 26% HPGe detector, as described above. Each sample was counted twice for a period of 10 min each [30]. The first measurement used for Na, Mg, and Al analysis may still contain some traces of F-17 (Table 1), which will interfere with carbon analysis. At the time of starting the second counting, there is a delay of 16 to 18 min from the end of irradiation, resulting in absence of F-17, and it is used exclusively for carbon analysis.

2.7. Quantification

The method of Ricci and Hahn [33] was used for quantification and shown in Equation (1). The stopping powers/ranges required for the calculations are taken from Ziegler et al. [34], applying Bragg's law to calculate the stopping power in compounds.

$$C_{\text{sample}} = \frac{A_{\text{sample}}}{A_{\text{standard}}} \times \left(\frac{R_{\text{standard}}}{R_{\text{sample}}} \right)_E \times C_{\text{standard}} \quad (1)$$

In Equation (1), C_{sample} and C_{standard} are mass concentrations of the sought element (carbon) in the sample (ppm) and standard. A_{sample} and A_{standard} are activities of sample and standard (counts/s/ μC /at end of irradiation), and R_{sample} and R_{standard} are ranges of sample and standard (g/cm^2) at the incident energy of 2.0 MeV.

Alternatively, one can also use stopping powers for analysis (Equation (2)), where S_{sample} and S_{standard} are stopping powers ($\text{MeV}/(\text{g}/\text{cm}^2)$).

$$C_{\text{sample}} = \frac{A_{\text{sample}}}{A_{\text{standard}}} \times \left(\frac{S_{\text{sample}}}{S_{\text{standard}}} \right)_E \times C_{\text{standard}} \quad (2)$$

For ranges/stopping power calculations, we used Bubastis glass from northern Egypt (Rosenow and Rehren [35]) as a reference, which has the following average composition (WH series): Si = 30.88%, Na = 13.28%, Ca = 5.09%, K = 0.38%, Mg = 0.56%, Al = 1.23%, Fe = 0.64%, Ti = 0.09%, Mn = 0.81%, Cl = 1.01%, S = 0.12%, and total oxygen = 44.14%.

The composition of the analysed glasses in this work need not tally with that of Bubastis. However, basically, they all consist of light elements, and small deviations in the concentrations of SiO_2 , Na_2O , MgO , CaO , etc., from glass to glass do not have any noticeable effect on range or stopping power calculations. Also, trace elements do not influence the calculations.

To provide an example, for 2.0 MeV deuterons, the ratio of ranges and stopping powers of Bubastis glass to carbon standard (100% carbon) are calculated and shown below:

$$\frac{S_{\text{bubastis}}}{S_{\text{carbon}}} = \left(\frac{0.1885 \left(\text{MeV} / \left(\frac{\text{mg}}{\text{cm}^2} \right) \right)}{0.2301 \left(\text{MeV} / \left(\frac{\text{mg}}{\text{cm}^2} \right) \right)} \right)_{E=2.0} = 0.8192 \quad (3)$$

$$\frac{R_{\text{carbon}}}{R_{\text{bubastis}}} = \left(\frac{0.005582 \left(\frac{\text{g}}{\text{cm}^2} \right)}{0.007050 \left(\frac{\text{g}}{\text{cm}^2} \right)} \right)_{E=2.0} = 0.7917 \quad (4)$$

One sees here a comparison of the ratio of stopping powers with ranges agreeing within 3%. This ratio is a “constant” and valid for carbon analysis in any glass of low-Pb type. (The analytical results shown in Table 2 are calculated using stopping power ratios.) For glasses with high Pb content at percentage level, separate calculations are required, which also include stopping power/range in Pb.

Table 2. Analytical results for C, Na, Mg, and Al in glass fragments and beads (all concentrations in weight %, unless otherwise stated. Errors: carbon: $\pm 10\%$ – 15% (for G1 and G2), carbon: $\pm 5\%$ – 7% (for B1–B5), Na, Mg, and Al: $\pm 10\%$). Note: oxygen interference (150 ppm) and carbon blank (50 ppm) are deducted from carbon results.

Sample	Colour	Concentration (wt %)			
		Carbon	Na	Mg	Al
Roman glass (G1)	blue	300 ppm	11.2	0.60	0.85
Roman glass (G2)	green	160 ppm	10.6	0.52	0.87
Roman bead (B1)	amber	0.65	5.4	0.27	0.32
Roman bead (B2)	pale amber	1.7	150 ppm	630 ppm	0.32
Roman bead (B3)	dark amber	2.2	11.1	1.12	0.93
Roman bead (B4)	dark brown	0.22	9.5	5.86	0.51
Roman bead (B5)	dark amber	0.94	8.1	0.99	1.02

3. Results and Discussion

The time elapsed from the end of irradiation to the beginning of counting of an irradiated sample is known as “decay time”. The gamma-ray spectrum of a Roman glass specimen G-1 irradiated with 2.0 MeV deuterons after decay times of 6 min is shown in Figure 3. Additionally, the gamma spectra of glass beads B-3 and B-5 are shown in Figure 4A,B, respectively. All these figures represent specially selected samples containing carbon at different concentration levels.

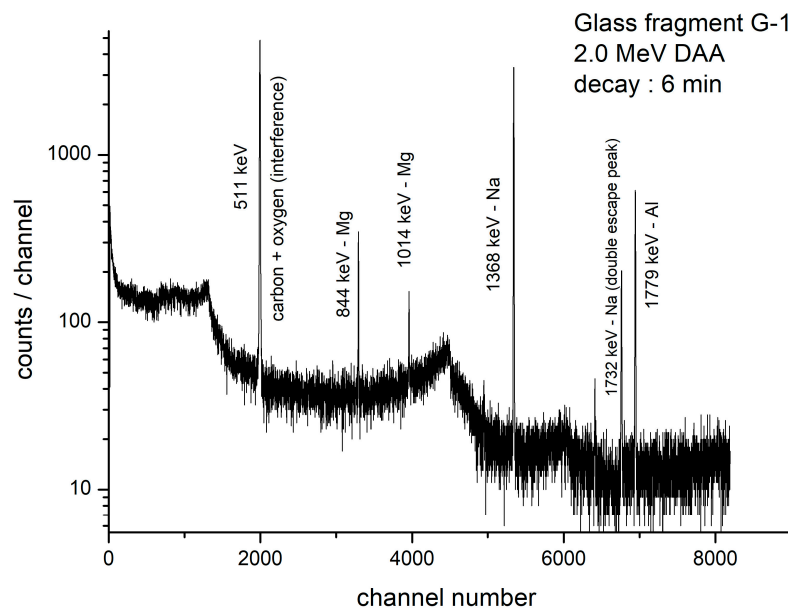


Figure 3. Gamma-ray spectrum of Roman glass G-1; decay time: 6 min, counting time: 590 s, charge: 16.2 μC (net counts in 511 keV peak = 51,460).

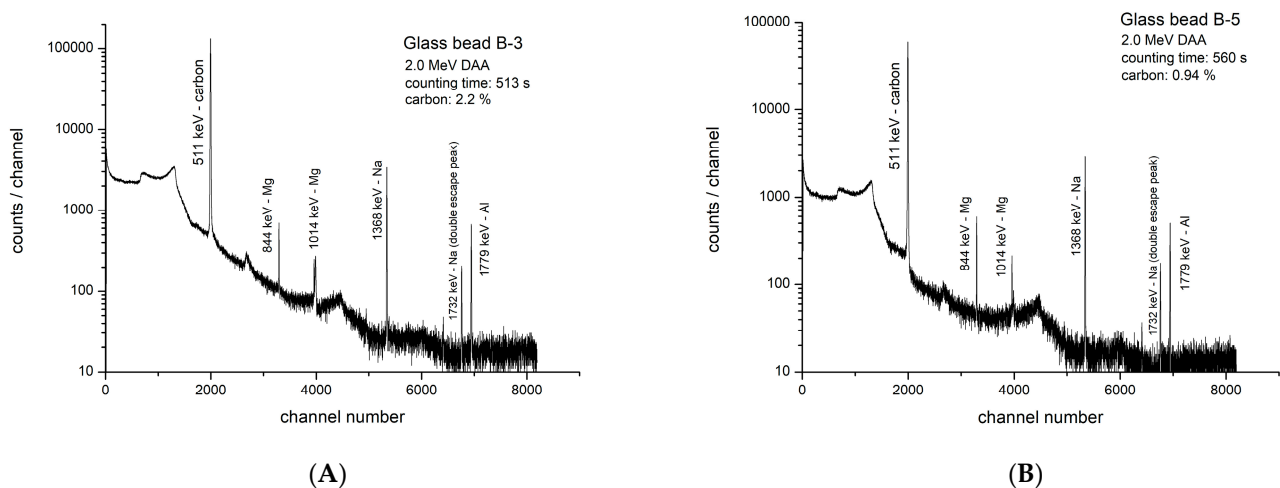


Figure 4. (A). Gamma-ray spectrum of Roman glass bead B-3, decay time: 380 s, counting time: 513 s, charge: 19.6 μC (net counts in 511 keV peak = 1,485,000). (B). Gamma-ray spectrum of Roman glass bead B-5; decay time: 470 s, counting time: 560 s, charge: 20.4 μC (net counts in 511 keV peak: 662,600).

In Figure 4A,B, the most intense peak (511 keV) is from N-13, revealing the “power” of DAA for carbon. Here, 1,485,000 counts (carbon: 2.2% in B3) and 662,600 counts (carbon: 0.94% in B5) were recorded in short counting times of 513 s and 560 s, respectively. Although Na is present at much higher concentrations than carbon in both beads, because of the very high sensitivity for the nuclear reaction with carbon, the N-13 peak is the strongest in the spectra.

The results for carbon in different glass fragments and beads are presented in Table 2, along with errors. This table also contains the results for Na, Mg, and Al, obtained in the first counting. Among various errors, the contribution from carbon standard is <1%. Other errors include photo-peak evaluation, formula used (stopping power/range) for quantification, errors in charge collection, positioning errors between sample and standard while placing on the detector head, etc.

3.1. Wood-Fuel Contamination and Carbon Role as a Colourant

The carbon concentration in glass fragments and beads varies between 160 ppm and 2.2%. It shows that fuel contamination did take place in the production of all the analysed glasses but was very low in glass fragments. It was higher (0.13%–0.44%) in the glasses analysed by us in a previous study [30].

The carbon observed in glass beads is at higher level, with the highest (2.2%) observed in glass B-3. It is to be expected that all these beads were also subjected to some level of fuel contamination. If we assume it was at a comparable level to that observed in G-1 and G-2, then the much higher concentration of carbon, especially in B3 and B5, has to be attributed to intentional addition of it to create a reducing atmosphere in the melt. This means that the ancient glass experts were aware of the role played by carbon in making amber glass.

The analysis of glass bead B-2 with a carbon concentration of 1.7% has to be separately discussed. The gamma-ray spectrum of B-2 (Figure 5A) looks very different from others. Here also, 1,413,400 counts were collected in 525 s under the 511 keV peak. However, only traces of Mg and Al are observed in the spectrum, and the Na peak is missing. To verify if Na is present at all, B-2 was counted again for 15,000 s after a decay of 48 h and shown in Figure 5B. Such a long counting, which is a standard procedure in NAA and CPAA, is applied to collect a statistically significant number of counts, provided that the nuclide (Na-24) representing the element (Na), present at a trace level, has a sufficiently long half-life (14.96 h). Because of 48 h decay, N-13, F-18, Mg-27, and Al-28 peaks are totally missing in Figure 5B. The extremely low concentration of Na at 150 ppm suggests this bead was probably made with plant ash additive. Such low Na values were noticed in plant-ash-based glasses from Syria [36]. Additional work is necessary to understand more about this bead.

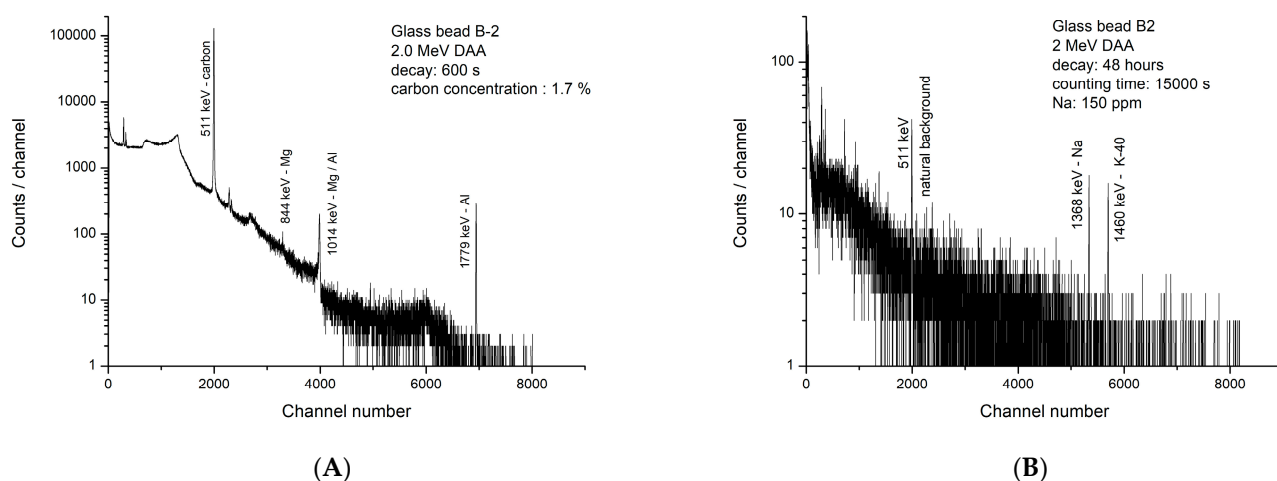


Figure 5. (A). Gamma-ray spectrum of Roman glass bead B-2; decay time: 600 s, counting time: 525 s, charge: 22.3 μC (net counts in 511 keV peak: 1,413,400). (B). Gamma-ray spectrum of Roman glass bead B-2; decay time: 48 h, counting time: 15,000 s (N-13 and F-18 are absent in 511 keV peak).

3.2. Carbon Contamination from Environment

While interpreting carbon results in glasses, one has to know the following:

In any laboratory, one can find traces of carbon coming from various sources, like dust, which contains several hydrocarbons, including CO_2 and CO molecules, whose origin can be automobiles, burning of wood and gas for heating houses, etc. [37]. Some of these molecules can become deposited on the surface of a glass specimen. The analyst must be aware of it, and a few ppm of carbon found in any archaeological glass is probably due to surface contamination in the laboratory. This is called “carbon blank” and can be estimated. It was estimated at CEMHTI by irradiating a high-purity quartz disc used as a beam monitor and found to be about 50 ppm [30]. We can assume that the blank calculated for quartz is applicable also to archaeological glasses.

To minimise this “carbon blank”, it is advisable to clean the samples shortly before analysis. The magnitude of blank can change from laboratory to laboratory depending on whether it is located in a residential or industrial area, proximity to road traffic, etc.

3.3. Nuclear Interferences

Carbon analysis is based on positron counting (N-13), which can be interfered by other positron emitters, like oxygen and silicon (Table 1), and is discussed below:

3.3.1. Oxygen Interference

The isotopes O-16 and O-17 are responsible for this interference. The interference caused by F-17 via O-16(d,n)F-17 is avoided by using the second counting for carbon, thus allowing for total decay of F-17.

However, the interference caused by F-18 via O-17(d,n)F-18 (half-life: 110 min) cannot be avoided. Luckily, although the total oxygen content of a glass is at a 40%–45% level, because of very low natural abundance of O-17 (0.038%), the production rate of F-18 via O-17(d,n)F-18 is very low, and, hence, the interference caused is low. It was found that, with 2 MeV deuterons, this interference contributes a “blank” of (150 ± 30) ppm in carbon analysis [30].

It must be emphasized that F-18 interference depends strongly on deuteron irradiation energy and irradiation time. Longer irradiation times should be avoided as they will unfavourably increase F-18 production to N-13 because of large differences in half-lives.

To confirm that F-18 is the only interfering positron emitter in carbon (N-13) analysis, additionally, we have conducted a decay curve analysis (Figure 6) of glass G-1, counted for 12 cycles at intervals of 10 min each. The contribution from N-13 to the total counts measured becomes nearly zero after eight to nine cycles of counting. Here, as expected, one sees only two components, namely N-13 (carbon) and F-18 (oxygen), confirming oxygen as the only element causing interference. (Decay curve analysis is a time-consuming process and is completed only initially while developing the analytical method. There is no need to conduct it in routine work).

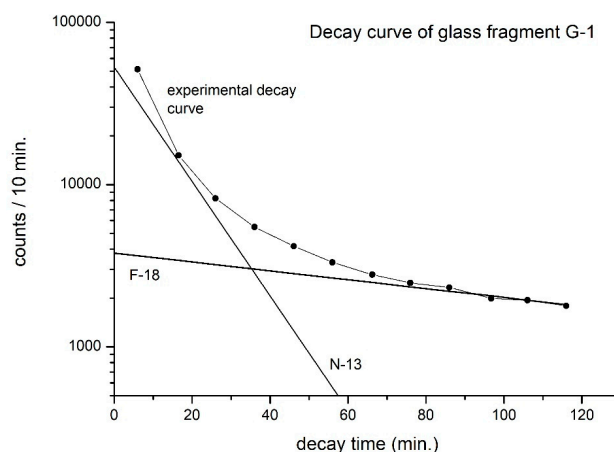


Figure 6. Decay curve analysis of Roman glass G-1. Charge: 16.2 μC (only N-13 and F-18 are viewed as decay components).

3.3.2. Silicon Interference

In a separate study, by irradiating a pure silicon target, we calculated the yield of P-30 and found that the silicon interference via Si-29(d,n)P-30 (Table 1) depends on sample decay time from the end of irradiation. As we use second counting for carbon analysis, there is a minimum decay of 17 to 18 min, which lowers Si interference to about 20 ppm in carbon analysis. As P-30 is a short-lived nuclide, this interference can be further reduced by increasing the decay time.

3.4. Subtraction of F-18 Interference and “Carbon Blank” from Carbon Results

The sum of F-18 interference (150 ppm) and “carbon blank” (50 ppm, applicable to CEMHTI) results in a total of 200 ppm, which has a significant influence on carbon results in G1 and G2. This interference has been subtracted from the results for carbon quoted in Table 2.

3.5. Detection Limit for Carbon with 2.0 MeV Deuterons

The detection limit depends on irradiation energy, irradiation, and counting conditions. Assuming that the minimum detectable activity is three times the square root of the background under a 511 keV peak, the “theoretical” detection limit for carbon in archaeological glass is 5 ppm under the current irradiation and measuring conditions [30]. However, this limit cannot be achieved because of the correction required at the 200 ppm level, as described above. This means that, with 2 MeV deuterons, carbon determination <200 ppm is not possible in any glass. Also, carbon concentrations <500 ppm must be carefully interpreted because of uncertainties in the magnitude of F-18 interference and “carbon blank” contribution from the analysing laboratory.

3.6. Selection of Deuteron Irradiation Energy for Carbon Analysis

It is advised to complete DAA by selecting a maximum of 2.0 MeV for deuterons. At >2 MeV, the sensitivity for carbon increases [30]. However, the number of positron emitters also increases, making it difficult to resolve the 511 keV peak (Figure 6) accurately. Already, at a deuteron energy of 2.5 MeV, calcium, which is normally present at 4 to 6% in glasses, interferes via $\text{Ca-40(d,}\alpha\text{)K-38}$ (half-life: 7.6 min) [19]. Also, oxygen interference caused by O-16 via O-16(d,n)F-17 (Table 1) becomes a serious problem with increasing deuteron energy [18,19].

3.7. Caution

One should be cautious while working with deuterons as several (d,n) reactions take place, with low-energy deuterons requiring neutron monitoring of the experimental area.

4. Conclusions

Some level of fuel contamination is observed in all analysed glass fragments and beads in the current study, similar to our previous work [30]. Basically, judged by the ancient furnace designs with wood as fuel, contamination of molten glass with waste gases was inevitable and its magnitude depended on the cleanliness and working conditions of the local glass workshops. We have shown that the DAA technique, with its extremely high sensitivity and good accuracy for carbon, is useful in understanding this problem.

Carbon observed at a percentage level in some beads clearly indicates that it was intentionally added as a component as the experts were aware of its role in creating amber and related glass shades.

DAA can be introduced in any PIXE/PIGE laboratory, and the generated gamma-ray spectra are simple to interpret. The total time taken for analysis, which includes irradiation (10 min), sample transfer time from the accelerator to the counting room, and two times counting (10 min each) is about 45 min (sometimes, there can be exceptions, with some samples requiring much longer counting time, like bead B-2). The method is non-destructive, and the analysed samples can be returned to the supplier after total decay of Na-24 activity, which will be about 10 days from the end of irradiation/analysis.

It must be stated that our current study is just the beginning of a new direction in archaeological glass analysis. As analysts, we have presented a simple nuclear technique for carbon quantification in archaeological glass and demonstrated its usefulness by analysing a few samples. It requires a larger study based on joint efforts by analysts and archaeologists to obtain a deeper understanding of this problem.

Author Contributions: C.S.S.—developed the concept. C.H. and C.S.S.—collected the samples. C.S.S. and T.S.—planned the experiments. T.S.—performed the irradiations and measurements. C.S.S.—conducted data analysis and drafted the original manuscript. T.S.—reviewed and edited the manuscript. O.W. and A.B.—provided technical assistance. All authors have read and agreed to the published version of the manuscript.

Funding: This research received no external funding.

Data Availability Statement: Not applicable.

Acknowledgments: The authors wish to thank Simon Breunig, 63906 Erlenbach, Germany for the supply of Roman glass beads.

Conflicts of Interest: The authors declare no conflict of interest.

References

1. Taylor, M.; Hill, D. Experiments in the reconstruction of Roman wood-fired glass working furnaces. *J. Glass Stud.* **2008**, *50*, 249–270.
2. Paynter, S. Experiments in the reconstruction of Roman wood-fired glass working furnaces: Waste products and their formation processes. *J. Glass Stud.* **2008**, *50*, 271–290.
3. Kistler, M.; Schmidt, C.; Padouvas, E.; Giebl, H.; Lohninger, J.; Ellinger, R.; Bauer, H.; Puxbaum, H. Odor, gaseous and PM₁₀ emissions from small scale combustion of wood types indigenous to central Europe. *Atmos. Environ.* **2012**, *51*, 86–93. [CrossRef]
4. Evtugina, M.; Alves, C.; Calvo, A.; Nunes, T.; Tarelho, L.; Duarte, M.; Prozil, S.O.; Evtuguin, D.V.; Pio, C. VOC emissions from residential combustion of Southern and mid-European woods. *Atmos. Environ.* **2014**, *83*, 90–98. [CrossRef]
5. Lauemann, E.; Putzgruber, G.; Götzinger, D. Problems and suggested solutions in the replication and operation of a glass furnace based on Roman remains: An experiment in glass production. *EXARC J.* 2016. Available online: <https://exarc.net/issue-2016-1/ea/problems-and-suggested-solutions-replication-and-operation-glass-furnace-based-roman-remains> (accessed on 25 July 2023).
6. Wiesenberg, F. Rohglas, Mosaikglas, Rippenschalen und römisches Fensterglas—Neues vom experimental-Archäologischen “Römischen” Glasofenprojekt im Archäologiepark Römische Villa Borg. In Proceedings of the Internationalen Symposiums zur Archäologie in der Großregion in der Europäischen Akademie Otzenhausen, Nonnweiler, Germany, 19–22 February 2015; pp. 265–272.
7. Tite, M.S.; Shortland, A.; Maniatis, Y.; Kavoussanaki, D.; Harris, S.A. The composition of the soda-rich and mixed alkali plant ashes used in the production of glass. *J. Archaeol. Sci.* **2006**, *33*, 1284–1292. [CrossRef]
8. Schibille, N.; Sterrett-Krause, A.; Freestone, I.C. Glass groups, glass supply and recycling in late Roman Carthage. *Archaeol. Anthropol. Sci.* **2017**, *9*, 1223–1241. [CrossRef]
9. Paynter, S.; Jackson, C.M. Mellow yellow: An experiment in amber. *J. Arch. Sci. Rep.* **2018**, *22*, 568–576. [CrossRef]
10. Bidegaray, A.I.; Godet, S.; Bogaerts, M.; Cosyns, P.; Nys, K.; Terry, H.; Ceglia, A. To be purple or not to be purple? How different production parameters influence colour and redox in manganese containing glass. *J. Arch. Sci. Rep.* **2019**, *27*, 101975. [CrossRef]
11. Reade, W.J.; Privat, K.L. Chemical characterisation of archaeological glasses from the Hellenistic site of Jebel Khalid, Syria by electron probe microanalysis. *Herit. Sci.* **2016**, *4*, 20. [CrossRef]
12. Cool, H.E.M. Glass and fuel. In *Fuel and Fire in the Ancient Roman World*; Veal, R., Leitch, V., Eds.; McDonald Institute for Archaeological Research: Cambridge, UK, 2019.
13. Segebade, C.; Weise, H.P.; Lutz, G.J. *Photon Activation Analysis*; Walter de Gruyter: Berlin, Germany, 1987.
14. Pierce, T.B.; Peck, P.F.; Henry, W.M. The rapid determination of carbon in steels by measurement of the prompt radiation emitted during deuteron bombardment. *Analyst* **1965**, *90*, 339–345. [CrossRef]
15. Debrun, J.L.; Barrandon, J.N.; Benaben, P. Irradiation of elements with $Z = 3$ to $Z = 42$ with 10 MeV protons and application to activation analysis. *Anal. Chem.* **1976**, *48*, 167–172. [CrossRef]
16. Engelmann, C. Utilisation des accélérateurs en analyse par activation, notamment pour la caractérisation des Matériaux purs. *J. Radioanal. Nucl. Chem.* **1980**, *58*, 29–47. [CrossRef]
17. Vandecasteele, C. *Activation Analysis with Charged Particles*; Ellis Horwood Limited: Chichester, UK, 1988.
18. Barthe, M.F.; Giovagnoli, A.; Blondiaux, G.; Debrun, J.L.; Tregooat, Y.; Barraud, J.Y. Fast analysis of oxygen in fluoride glasses (ZBLAN) by charged-particle activation [O-16(d,n)F-17]. *Nucl. Instrum. Methods Phys. Res.* **1990**, *45*, 105–106. [CrossRef]
19. Sastri, C.S.; Blondiaux, G.; Hoffmann, P.; Ortner, H.M.; Petri, H. Oxygen determination in calcium fluoride by deuteron activation analysis, Fres. *J. Anal. Chem.* **2000**, *366*, 218–220.
20. Sastri, C.S.; Banerjee, A.; Sauvage, T.; Courtois, B.; Duval, F. Application of 12 MeV proton activation to the analysis of archaeological specimens. *J. Radioanal. Nucl. Chem.* **2016**, *308*, 241–249. [CrossRef]
21. Qaim, S.M. *Medical Radionuclide Production, Science and Technology*; Walter de Gruyter: Berlin, Germany; Boston, MA, USA, 2020.
22. Pupillo, G.; Mou, L.; Manenti, S.; Groppi, F.; Esposito, J.; Haddad, F. Nuclear data for light charged particle induced production of emerging medical radionuclides. *Radiochim. Acta.* **2022**, *110*, 689–706. [CrossRef]
23. Albert, P.; Chaudron, G.; Sue, P. Microdosage par voie chimique du carbone dans le fer irradié par le deutons. *Bull. Soc. Chim. Fr.* **1953**, *20*, 97–102.

24. Winchester, J.W.; Buttino, M.L. Determination of carbon, oxygen and silicon in solids by activation analysis with 15 MeV deuterons. *Anal. Chem.* **1961**, *33*, 472–473. [[CrossRef](#)]
25. Koemmerer, C. Etude sur l' Incorporation du Carbone et de l' Oxygene au Cours de l' Elaboration de GaAs, en Utilisant l' Analyse par Activation au Moyen de Particules Chargees de Basse Energie. Ph.D. Thesis, University of Orleans, Orleans, France, 1982.
26. Misdaq, M.A.; Blondiaux, G.; Bordes, N.; Giovagnoli, A.; Valladon, M.; Wei, L.C.; Hage Ali, M.; Maggiore, C.J.; Debrun, J.L. Recent progress in the study of semiconductors using charged particle activation. *J. Radioanal. Nucl. Chem.* **1987**, *110*, 441–449. [[CrossRef](#)]
27. Sastri, C.S.; Blondiaux, G.; Petri, H. Trace determination of carbon, sodium, magnesium and aluminum in metals and ceramic materials by low energy deuteron activation analysis. *Nucl. Instrum. Methods Phys. Res.* **1997**, *124*, 558–566. [[CrossRef](#)]
28. Albert, P.; Blondiaux, G.; Debrun, J.L.; Giovagnoli, J.; Valladon, M. Activation cross-sections for elements from lithium to Sulphur. In *Handbook on Nuclear Activation Data*; Technical Report Series no. 273; IAEA: Vienna, Austria, 1987.
29. Sastri, C.S.; Sauvage, T.; Blondiaux, G.; Wendling, O.; Bellamy, A.; Humburg, C. Analysis of Na, Mg, Al and Cl in archaeological glass and pottery: Comparison of PIGE with low energy deuteron activation analysis. *J. Radioanal. Nucl. Chem.* **2020**, *324*, 159–167. [[CrossRef](#)]
30. Sastri, C.S.; Sauvage, T.; Blondiaux, G.; Wendling, O.; Bellamy, A.; Humburg, C. Analysis of carbon in archaeological glass and pottery by low energy deuteron activation technique. *J. Radioanal. Nucl. Chem.* **2021**, *320*, 889–897. [[CrossRef](#)]
31. Sastri, C.S.; Sauvage, T. Fuel contamination problems in Roman wood-fired glass furnaces: Carbon determination in Roman glass by deuteron activation technique. Presented at the International Conference METROARCHAEO 2022, Cosenza, Italy, 19–21 October 2022.
32. Chu, S.Y.F.; Ekström, L.P.; Firestone, R.B. The Lund/LBNL Nuclear Data Search. Version 2.0. 1999. Available online: <http://www.nucleardata.nuclear.lu.se/toi/> (accessed on 25 July 2023).
33. Ricci, E.; Hahn, R.L. Sensitivities for activation analysis of 15 light elements with 18 MeV Helium-3 particles. *Anal. Chem.* **1967**, *39*, 794–797. [[CrossRef](#)]
34. Ziegler, J.F.; Ziegler, M.D.; Biersack, J.P. 2008, Version SRIM-2008.04. Available online: <http://www.srim.org> (accessed on 25 July 2023).
35. Rosenow, D.; Rehren, T. Herding cats: Roman to late antique glass groups from Bubastis, northern Egypt. *J. Arch. Sci.* **2014**, *49*, 170–184. [[CrossRef](#)]
36. Barkoudab, Y.; Henderson, J. Plant ashes from Syria and the manufacture of ancient glass: Ethnographic and scientific aspects. *J. Glass Stud.* **2006**, *48*, 297–321.
37. Vicente, E.D.; Vicente, A.; Nunes, T.; Calvo, A.; del Blanco-Alegre, C.; Oduber, E.; Castro, A.; Fraile, R.; Amato, F.; Alves, C. House hold dust: Loadings and PM₁₀-bound plasticizers and polycyclic aromatic hydrocarbons. *Atmosphere* **2019**, *10*, 785. [[CrossRef](#)]

Disclaimer/Publisher's Note: The statements, opinions and data contained in all publications are solely those of the individual author(s) and contributor(s) and not of MDPI and/or the editor(s). MDPI and/or the editor(s) disclaim responsibility for any injury to people or property resulting from any ideas, methods, instructions or products referred to in the content.